EL SEVIER

Contents lists available at ScienceDirect

Earth and Planetary Science Letters

journal homepage: www.elsevier.com/locate/epsl





Magnetization and age of ca. 544 Ma syenite, eastern Canada: Evidence for renewal of the geodynamo

Tinghong Zhou ^a, Mauricio Ibañez-Mejia ^b, Richard K. Bono ^c, Rory D. Cottrell ^a, Wouter Bleeker ^d, Kenneth P. Kodama ^e, Wentao Huang ^f, Eric G. Blackman ^g, Francis Nimmo ^h, Aleksey V. Smirnov ^{i,j}, John A. Tarduno ^{a,g,k,*}

- ^a Department of Earth and Environmental Sciences, University of Rochester, Rochester, NY 14627, USA
- ^b Department of Geosciences, University of Arizona, Tucson, AZ 85721, USA
- ^c Department of Earth, Ocean and Atmospheric Science, Florida State University, Tallahassee, FL 32306, USA
- ^d Geological Survey of Canada, 601 Booth Street, Ottawa K1A 0E8, Canada
- ^e Department of Earth and Environmental Sciences, Lehigh University, Bethlehem, PA 18015, USA
- f State Key Laboratory of Tibetan Plateau Earth System, Environment and Resources (TPESER), Institute of Tibetan Plateau Research, Chinese Academy of Sciences, Beijing 100101, China
- g Department of Physics and Astronomy, University of Rochester, Rochester, NY 14627, USA
- ^h Department of Earth and Planetary Sciences, University of California, Santa Cruz, CA 95064, USA
- Department of Geological and Mining Engineering and Sciences, Michigan Technological University, Houghton, MI 49931, USA
- ^j Department of Physics, Michigan Technological University, Houghton, MI 49931, USA
- ^k Laboratory for Laser Energetics, University of Rochester, Rochester, NY 14623, USA

ARTICLE INFO

Editor: J. Badro

Dataset link: https://doi.org/10.6084/m9.figshare.24639186

Keywords: single crystal paleointensity core processes inner core nucleation Ediacaran paleomagnetism

ABSTRACT

The ca. 565 Ma Ediacaran geodynamo was highly unusual, producing an ultralow field 10 times weaker than present-day value of 8 x 10^{22} A m². A ~5 times rise in field strength is seen in time-averaged single crystal paleointensity data of ca. 532 Ma Early Cambrian anorthosites of Oklahoma (USA). The field increase could record the onset of inner core nucleation predicted by thermal evolution and numerical dynamo models. Here, we examine the renewal of the geodynamo through zircon U-Pb geochronology and single crystal paleointensity studies of plagioclase from the Chatham-Grenville syenite intrusion in the Grenville Province (Canada). U-Pb data indicate a ca. 544 Ma age and Thellier single crystal paleointensity data yield field strengths of 2.3 \pm 0.6 x 10^{22} A m². The new single crystal paleointensity data further support an increase in field intensity near the Ediacaran-Cambrian transition, consistent with latent heat of crystallization and release of light elements providing new energy sources to power the geodynamo upon the onset of inner core nucleation. Moreover, our new results suggest that plagioclase from syenites can yield valuable records of the geodynamo.

1. Introduction

Understanding the evolution of paleomagnetic field strength in the Precambrian is important because this history could contain clues to the onset of inner core nucleation (ICN), and how the inner core grew. Some numerical geodynamo models call for an Ediacaran age for ICN (Driscoll, 2016) and a field approaching the weak field state where core kinetic energy exceeds magnetic energy. The independent discovery of a time-averaged ultralow field intensity by Bono et al. (2019) using single crystal paleointensity (SCP; Tarduno et al., 2006) analyses of feldspars and pyroxenes from ca. 565 Ma anorthosites of the Sept-Îles Mafic In-

trusive Suite (Higgins, 2005) of northern Quebec (Canada) heightened attention on the Ediacaran as a potential time of ICN. The paleomagnetic dipole moment reported by Bono et al. (2019) of 0.7 \pm 0.3 x 10^{22} A m^2 is ten times weaker than that of the present-day field.

Soon after the first report of the time-averaged field ultralow strength (Bono et al., 2019), similar instantaneous ultralow values were reported from Ediacaran-age dikes and lavas (Shcherbakova et al., 2020; Thallner et al., 2021a), such that the data defining this unusually weak field now come from several localities on Laurentia and Baltica. The model prediction of field strength at the time of ICN, however, is not just an ultralow paleointensity. Following this weak field,

E-mail address: john@earth.rochester.edu (J.A. Tarduno).

https://doi.org/10.1016/j.epsl.2024.118758

Received 8 December 2023; Received in revised form 3 May 2024; Accepted 4 May 2024 Available online 25 May 2024

0012-821X/© 2024 The Author(s). Published by Elsevier B.V. This is an open access article under the CC BY-NC-ND license (http://creativecommons.org/licenses/by-nc-nd/4.0/).

^{*} Corresponding author.

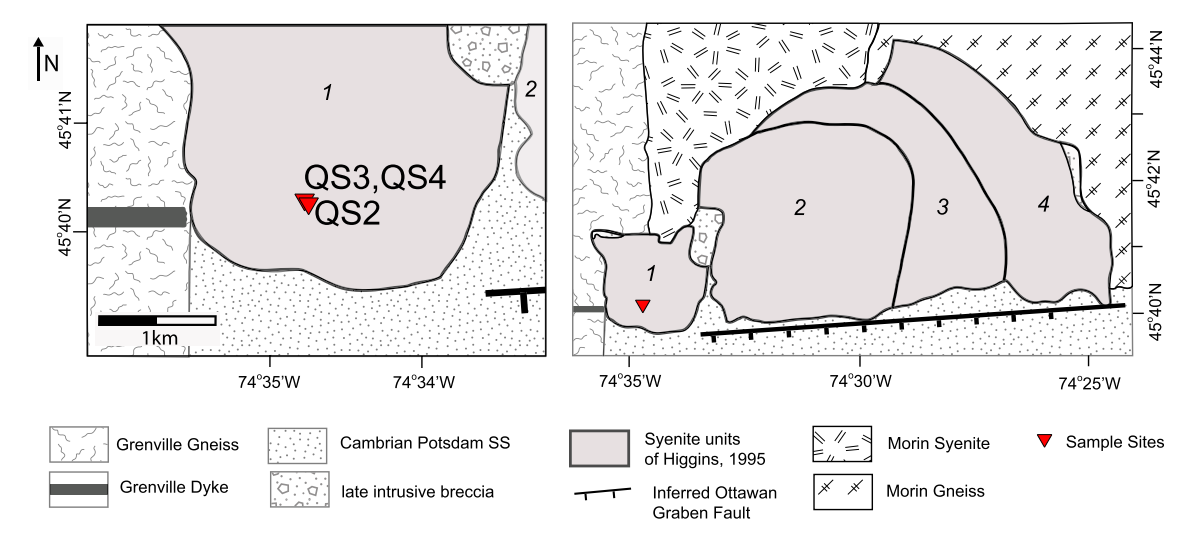


Fig. 1. Chatham-Grenville stock sampling sites. Sketch map modified from Higgins (1985) and Lloyd et al. (2022). Unit numbers from Higgins (1985) are as follows: 1. Noncumulate syenite with modal quartz <5%; 2. Cumulate to noncumulative syenite (0 to 20% modal quartz); 3. Granite with modal quartz of 25%; 4. Granite with modal quartz of 30%.

the strength should rapidly increase as new sources of energy from latent heat of crystallization and buoyancy driven by the expulsion of light elements become available to power the geodynamo. But, identifying any such increase in field strength was prohibited by a lack of reliable latest Ediacaran to early Cambrian paleointensity data at the time of the studies that first recognized the Ediacaran ultralow fields.

Zhou et al. (2022) reported the first time-averaged SCP values for the early Cambrian from 532.49 ± 0.12 Ma (U-Pb zircon age) (Wall et al., 2021) anorthosites of the Glen Mountains Layered Complex (Hanson et al., 2013) of the Wichita Mountains (Oklahoma). The paleomagnetic dipole moment reported by Zhou et al. (2022) is $3.5 \pm 0.9 \times 10^{22} \text{ A m}^2$, some 5 times higher than that of the Sept-Îles Mafic Intrusive Suite. Zhou et al. (2022) concluded that this increase was the, up to this point, undefined paleointensity signal of new energy sources accompanying ICN. Based on these data, the age of ICN was constrained to ca. 550 Ma, and the critical core transition between the innermost inner core to outermost inner core boundary defined by seismic anisotropy (e.g., Stephenson et al., 2021) was estimated to have formed at ca. 450 Ma, assuming that inner core growth was driven by a constant heat flux (Nimmo, 2015). Other ages continue to be proposed for ICN (Zhang et al., 2022), but none has the concurrence of geodynamo and thermal model predictions (Driscoll, 2016), near weak-field observations (Bono et al., 2019; Shcherbakova et al., 2020; Thallner et al., 2021a), and a relatively rapid increase in field strength (Zhou et al., 2022) that characterize the Ediacaran/earliest Cambrian transition (Li et al., 2023). In model predictions of Davies et al. (2022), this remains the most probable time for ICN.

Herein, we investigate the proposed renewal of the geodynamo through studies of the Chatham-Grenville syenite intrusion (Higgins, 1985) in the Grenville Province (Canada), part of magmatism that has previously been assigned Ediacaran or Cambrian ages (Malka et al., 2000; McCausland et al., 2007; see also Bleeker et al., 2011, for general geological setting). We first conduct new zircon U-Pb geochronology analyses and single crystal paleointensity studies on plagioclase from the syenite. We then discuss these data with respect to prior age and paleointensity results. We conclude with the implications for the geodynamo and inner core nucleation.

2. Chatham-Grenville syenite stock geochronology

Three samples (QS-2, QS-3, and QS-4) from the Chatham-Grenville syenite stock were collected from a fresh quarry exposure [in Units 1 mapped by Higgins (1985)] as part of the University of Rochester's on-

going studies in the region (Bono and Tarduno, 2015; Bono et al., 2019; Methods) (Fig. 1). Zircon crystals from all three samples were abundant and large, with sizes ranging from $\sim\!200$ to 500 μm on average. Zircon crystals were mostly unzoned in cathodoluminescence (CL) response, while approximately one third of crystals from all samples showed evidence of oscillatory zoning typical of magmatic zircon (Supplementary Figs. 1–3). Approximately 50 individual U-Pb spot measurements were performed in each sample, targeting areas of the zircon with oscillatory zoning and/or homogeneous CL response and away from any apparent correct

All individual spot analyses (Fig. 2; see also Section 5.2 Methods) yielded concordant results within uncertainty, with calculated U concentrations ranging from 18 to 317 $\mu g/g$ and a median of 76 $\mu g/g$. Weighted means (see Methods for uncertainty notation) for the three samples studied here yielded $^{206}\text{Pb}/^{238}\text{U}$ ages undistinguishable within uncertainty of 546.2 \pm 2.8/5.9 Ma (2 σ , n=42, MSWD=0.55), 542.3 \pm 3.0/5.9 Ma (2 σ , n=46, MSWD=0.35), and 543.8 \pm 2.8/5.8 Ma (2 σ , n=47, MSWD=0.42) for QS-2, QS-3, and QS-4, respectively (Fig. 2). The weighted mean age of all data yields 544.1 \pm 1.7/5.4 Ma (2 σ , n=135, MSWD=0.42).

3. Chatham-Grenville SCP analyses

Whole rock samples of syenite are typically dominated by multidomain (MD) magnetic grains and are problematic paleomagnetic recorders. The SCP technique (Cottrell and Tarduno, 1999, 2000; Tarduno et al., 2006; Tarduno, 2009) directly addresses this by targeting silicates with minute magnetic inclusions, smaller than the MD state. Comparative studies of single plagioclase crystals and whole rocks document the superior recording fidelity of the former (Cottrell and Tarduno, 2000). Further comparative studies of silicates confirm both the near ideal behavior of some plagioclase and nonideal behavior of some other mafic silicates phases common in whole rocks (Dunlop et al., 2005).

Rare plagioclase crystals were identified and separated from sample QS-3 and analyzed using SCP techniques (Tarduno et al., 2006; Methods). Magnetic hysteresis analyses of such crystals showed weak signals with variable behavior (Fig. 3). Some show wide loops indicating single domain (SD) components (Fig. 3a,c) supported by the central ridge of first order reversal curves (Fig. 3b). Others have more nominal pseudosingle domain (PSD) behavior (Fig. 3d) with narrowness at low fields that could be a sign of superparamagnetic grains. The latter is also hinted at by where one sample (a of Fig. 3) falls on a Day plot

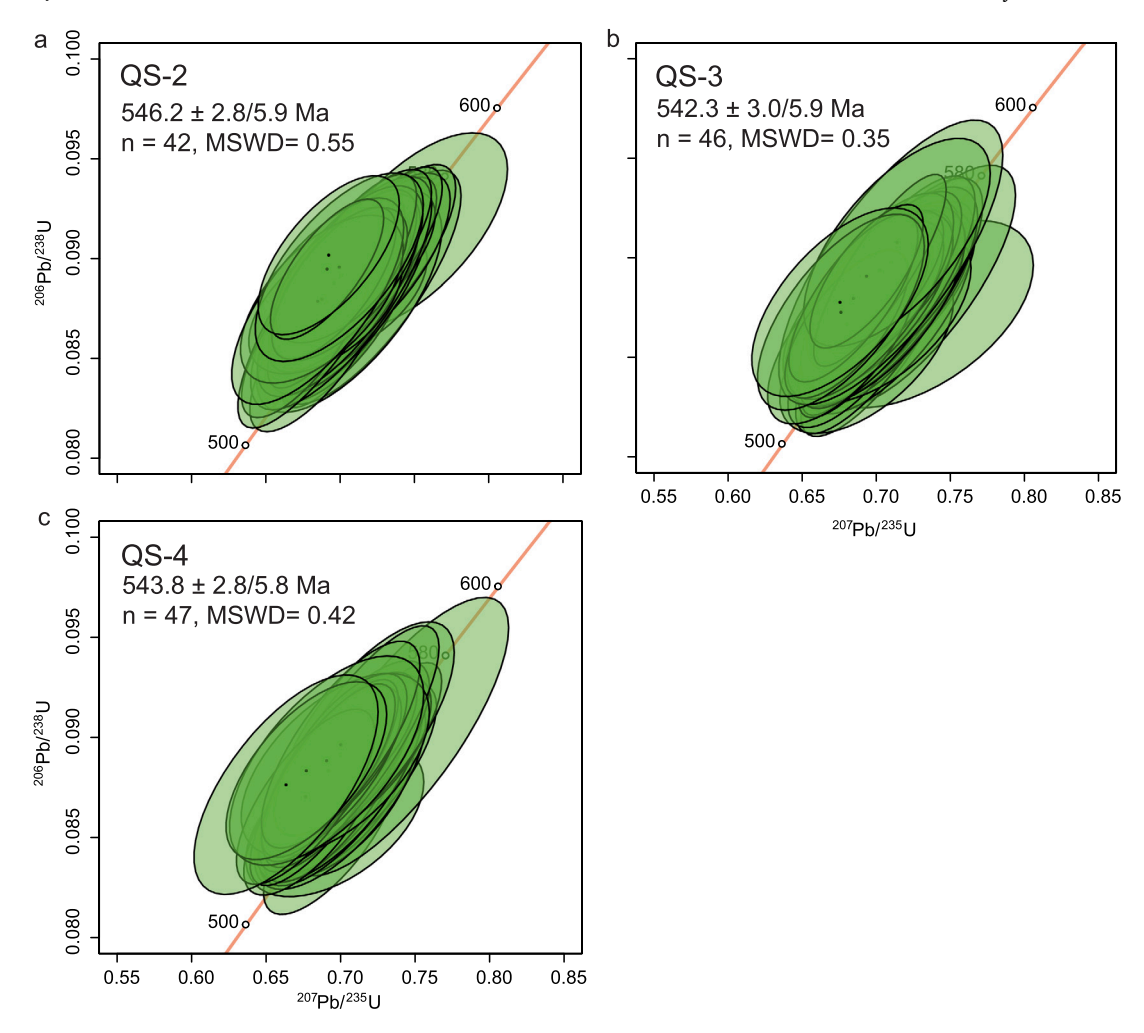


Fig. 2. Zircon U-Pb Geochronology from Chatham-Grenville stock. **(a)** Concordia plot of zircon ²⁰⁶Pb/²³⁸U versus ²⁰⁷Pb/²³⁵U data for sample QS2. **(b)** Data for QS3. **(c)** Data for QS4.

(Fig. 3e). The hysteresis data from crystal "d" suggests that magnetic inclusions in some of these plagioclases could be dominated by somewhat larger grains than the fine exsolved needles seen in some anorthosite plagioclase (e.g. Bono et al., 2019; Zhou et al., 2022). Scanning electron microscope studies (Methods) confirm this inference (Fig. 3f). Although titanomagnetite needle-shaped grains are observed in a crystal having a SD-like magnetic hysteresis curve ("a" of Fig. 3), others particles in the same crystal have lower aspect ratios and larger sizes (a few microns). Many of these larger grains have intergrown areas of relatively lower and higher Ti. An elongated grain without titanium, presumed to be magnetite, was also observed.

To obtain an initial estimate of paleointensity and assess unblocking, total thermoremanent magnetization (TTRM) experiments were performed (Tarduno et al., 2012), whereby a crystal's natural remanent magnetization (NRM) was thermally demagnetized using a CO₂ laser (Tarduno et al., 2007). A total TRM was imparted by heating the sample to 560 o C and cooling in the presence of a 60 μ T field. Next, the sample was stepwise demagnetized; the ratio of the NRM lost to TRM gained over the highest unblocking temperature range with stable magnetizations (500-560 o C in this case) was used to estimate the paleointensity (in general, orthogonal vector plots of the thermal demagnetization of the syenite plagioclase crystals show a break in slope at temperatures of 475-500 o C after which the vector trends to the origin). Two experiments yielded values of 12.2 \pm 0.7 μ T and 16.6 \pm 0.9 μ T (Fig. 4).

Next, SCP Thellier-Coe analyses with partial thermoremanent magnetization (pTRM) checks (hereafter, referred to as Thellier analyses;

Methods) were conducted on plagioclase crystals from QS-3 using an applied field of 30 and 15 μT , the latter closer to the paleointensity obtained by the TTRM experiments (Fig. 5, Supplementary Table 2). Five experiments yielded data passing acceptance criteria (Methods, Supplementary Table 2) and a mean paleointensity of 9.9 \pm 2.4 μT . Given the possibility that the plagioclase is dominated by inclusions in the PSD state, a cooling correction (e.g., Halgedahl et al., 1980; Yu, 2011) may not be needed; in addition, the lack of dominant needle-like inclusions implies that anisotropy corrections will similarly be minor. We assume a paleolatitude of $\sim\!16^o$ based on the expected inclination of $\sim\!30^o$ derived from the QS3 site location and the paleopole of Lloyd et al. (2022). The Thellier results yield a virtual dipole moment of 2.31 \pm 0.55 x10²² A m². Because of the relatively slow cooling of the syenite, this value should also represent the time-averaged field.

4. Discussion

4.1. Age of emplacement of the Chatham-Grenville stock

We first discuss results from the Mont Rigaud intrusion because, as described below, these data have been used to infer ages for the Chatham-Grenville stock, assuming these separate stocks represent the same magmatic event. Malka et al. (2000) presented zircon U-Pb data from what they mapped as Unit 1 (feldspar-hornblende syenite) and Unit 3 (granite) of the Mont Rigaud stock using isotope dilution-thermal ionization mass spectrometry (ID-TIMS) of air-abraded aliquots. Despite the air-abrasion pre-treatment, zircon U-Pb results were moderately to

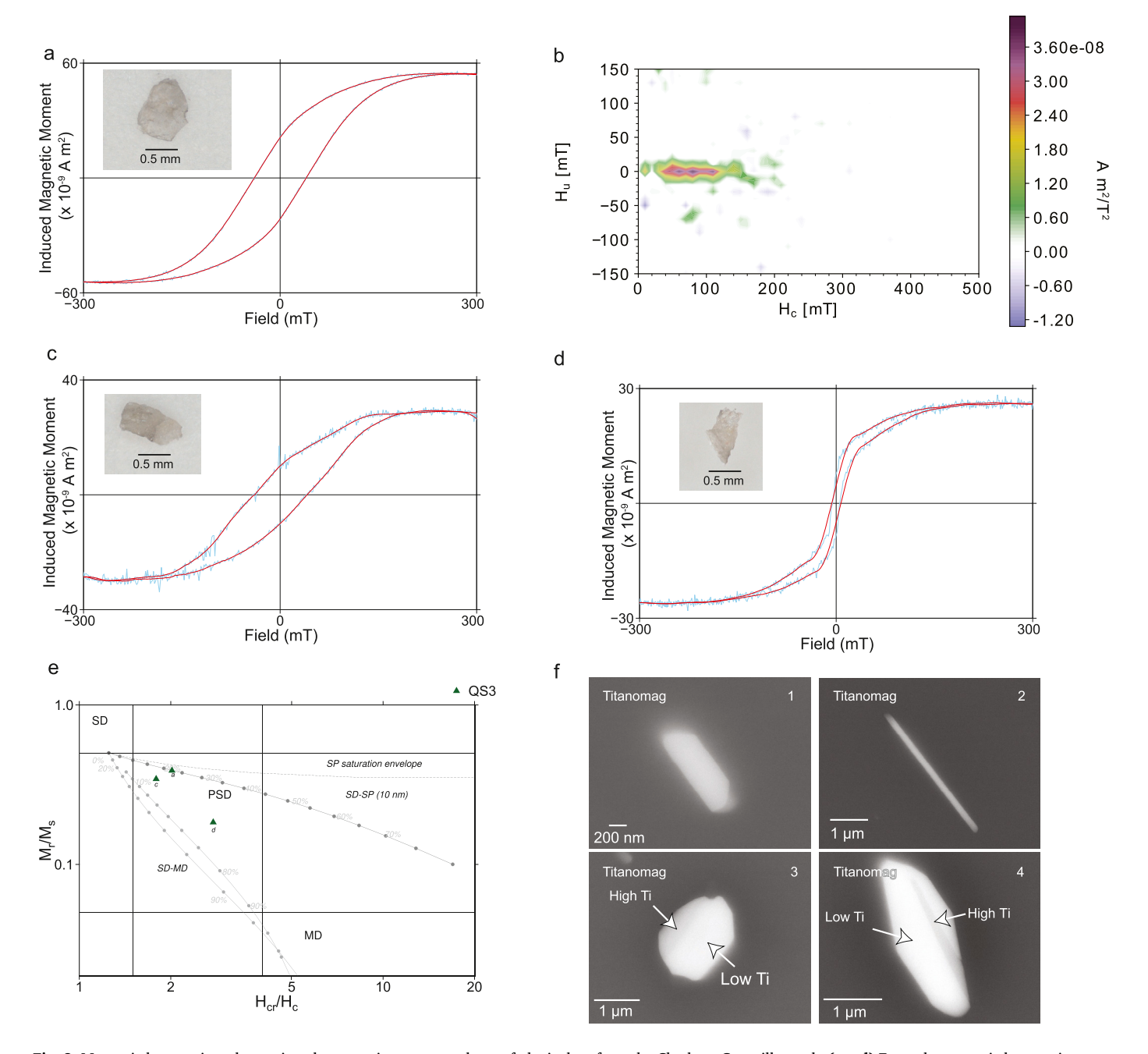


Fig. 3. Magnetic hysteresis and scanning electron microscope analyses of plagioclase from the Chatham-Grenville stock. (**a,c,d**) Example magnetic hysteresis curves from plagioclase; respective crystal measured shown in the inset. (**b**) First Order Reversal Curve Diagram for crystal shown in (a). Smoothing parameters (Methods): Sc0 = Sc1 = Su0 = Su1 = 2; $\lambda_x = \lambda_y = 0.1$. (**e**) Day plot with mixing curves from Dunlop (2002). (**f**) Scanning electron microscope backscatter images in 20 keV: 1. elongated titanomagnetite particle with an aspect ratio (length/width) of 2.7; 2. elongated titanomagnetite needle with an aspect ratio of 24.6; 3. titanomagnetite with high Ti and low Ti exsolution patterns, aspect ratio 2.7.

strongly discordant. Malka et al. (2000) reported upper intercept ages from discordia regressions of 556 $^{+15}_{-12}$ Ma for Unit 1 and 564 $^{+10}_{-8}$ Ma for Unit 3, which overlap within uncertainty and were thus interpreted as reflecting an age of emplacement ca. 560 Ma for Mont Rigaud.

McCausland et al. (2007) later performed 40 Ar/ 39 Ar analyses of hornblende from both the Mont Rigaud and the Chatham-Grenville stocks. A site in Unit 1 (Higgins, 1985) of the Chatham-Grenville stock, closest to a dike studied by Lloyd et al. (2022), yielded contrasting ages. A total gas age of 533.1 \pm 1.5 Ma was reported from one hornblende, but without a robust plateau. Another hornblende yielded a plateau age of 554.6 \pm 1.6 Ma and the authors report this result was replicated, but they ultimately reject these data because of increased apparent ages

and higher Ca/K, Cl/K values seen in the final degassing steps. Instead, McCausland et al. (2007) selected plateau ages from two other sites in the Chatham-Grenville stock, far from the dike sampled by Lloyd et al. (2022) [CG14, syenite Unit 2 of Higgins (1985) and CG31, granite unit 3 of Higgins (1985)], and one site in the Mont Rigaud stock [MR10, syenite Unit 2 of Malka et al. (2000)], to calculate an age of 531.9 ± 1.4 Ma which was reported as a weighted mean of five hornblende plateau ages. Noting the discordance of the U-Pb data of Malka et al. (2000), McCausland et al. (2007) argued that their hornblende 40 Ar/ 39 Ar dates represent a more accurate age for the combined Chatham-Grenville/Mont Rigaud intrusions. However, the lack of inverse isochron plots and details regarding how the air corrections for

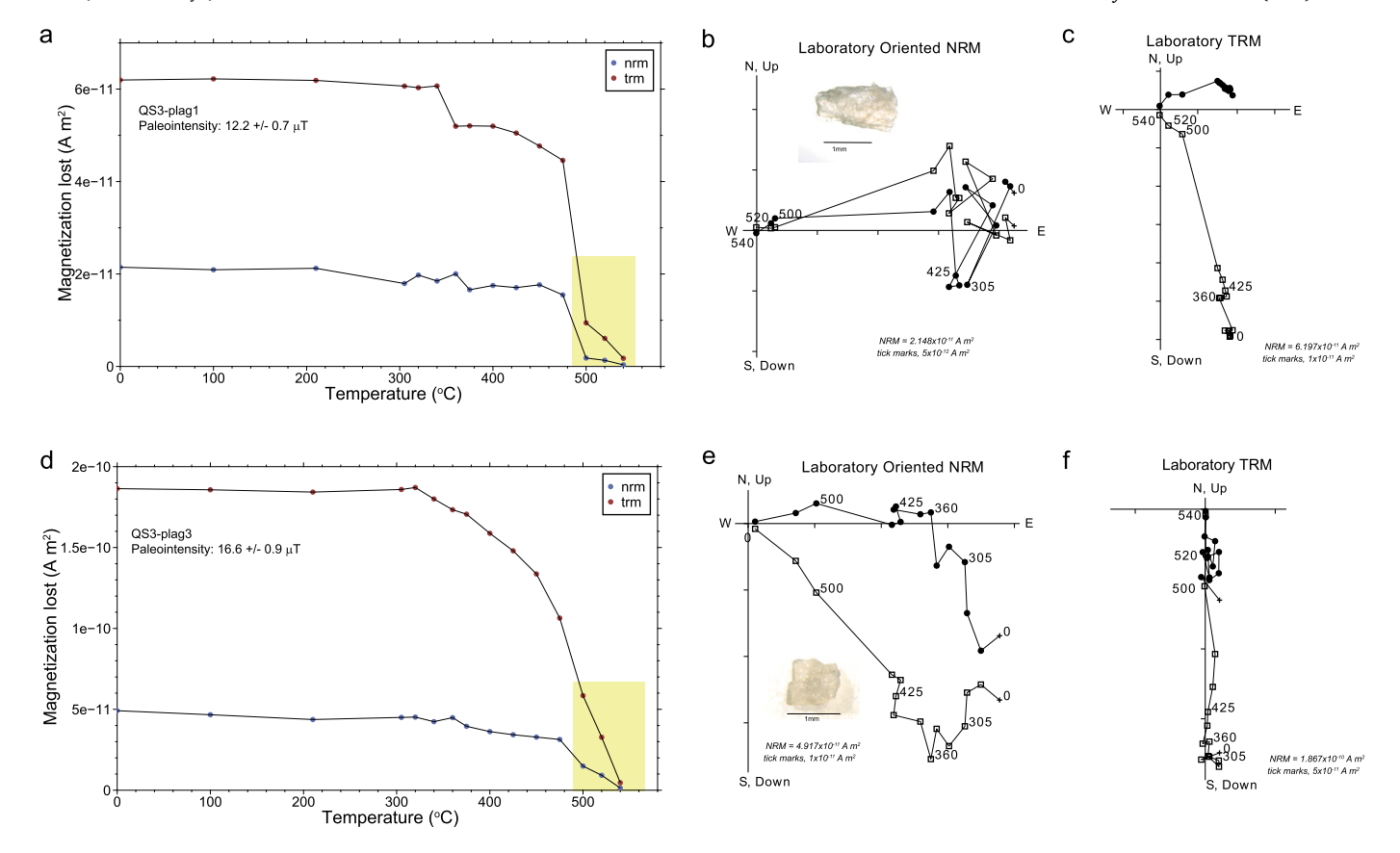


Fig. 4. Single crystal paleointensity data from Chatham-Grenville stock: Total Thermoremanent Magnetization experiments. **(a)** Natural remanent magnetization (NRM) demagnetization versus total thermoremanent magnetization (TTRM) demagnetization for crystal QS3-plag1. **(b)** Orthogonal vector plot of thermal demagnetization of NRM (crystal is unoriented). Temperatures shown are in °C. Crystal measured (i.e., QS3-plag1) shown as inset. Solid circles: horizontal projection of the magnetization, open box: vertical projection of the magnetization of TTRM. Temperatures shown are in °C. Solid circles: horizontal projection of the magnetization, open box: vertical projection of the magnetization. **(d, e, f)** NRM, TRM demagnetizations, orthogonal vector plot of NRM demagnetization and orthogonal vector plot of TTRM demagnetization for crystal QS3-plag3 following a,b,c, respectively.

the interpreted age spectra were made, make the accuracy of the McCausland et al. (2007) $^{40}{\rm Ar}/^{39}{\rm Ar}$ results difficult to evaluate.

In this study, we have obtained new zircon U-Pb geochronology from three syenite samples. In contrast to the previous U-Pb data reported by Malka et al. (2000), all individual spot dates (n=135) obtained from our samples are concordant and overlap within analytical uncertainty. The ²⁰⁶Pb/²³⁸U weighted mean ages from our samples, which range from 542.3 ± 3.0 Ma to 546.2 ± 2.8 Ma (considering internal uncertainties only), are younger than the upper intercepts of discordant zircon data reported by Malka et al. (2000) but older than the hornblende ⁴⁰Ar/³⁹Ar results of McCausland et al. (2007). We note that the zircons we measured were not thermally annealed and/or chemically abraded prior to analysis, and therefore a subdued effect of Pb loss affecting the $^{206}\text{Pb}/^{238}\text{U}$ dates cannot be fully ruled out. However, given the very low U concentrations determined in the zircon we analyzed (median U of 76 µg/g), and the systematic overlap of all U-Pb analyses conducted, we consider it unlikely that these zircons could have accumulated sufficient radiation damage to enable Pb remobilization.

The U-Pb system in zircon has slower diffusion kinetics than K-Ar (and hence Ar-Ar) in amphibole and therefore records higher temperatures, i.e., $\sim\!900\,^{\circ}\text{C}$ versus $\sim\!500\,\text{C}^{\circ};$ given the petrology and field relations indicating shallow crustal emplacement and differentiation of the stocks, it is likely they cooled on a million-year time scale close to the age indicated by our U-Pb data. For this reason, and the aforementioned concerns over Ar diffusion and lack of details regarding trapped gas corrections for the published plateau dates, we conclude that the U-Pb data provide the best estimate for the magnetization age.

${\it 4.2. \ Paleo intensity\ recorded\ by\ the\ Chatham-Grenville\ syenite\ stock}$

As noted previously, syenite bulk rocks are problematic for paleomagnetic analyses in general (e.g., Prevot et al., 2000; Tarduno and Smirnov, 2001), but our results indicate that progress can be made through SCP analyses of rare plagioclase crystals. While the Thellier paleointensity estimates together yield an acceptable paleointensity confidence interval of $\pm 2.4~\mu T$, we note that some of the individual determinations have non-overlapping confidence intervals. The source of this variation is unknown, but it is possible that specimen specific magnetic grain size variation, discussed in Section 3, is adding scatter that is not fully captured by standard uncertainty estimates for the individual determinations. Notwithstanding this variation, we note the agreement of the mean with the paleointensity trend predicted by Zhou et al. (2022) (Fig. 6) which we discuss further in Section 4.4 below.

4.3. Did the latest Ediacaran/earliest Cambrian field have large variations on tens of thousands to hundreds of thousands of years?

While our new paleointensity value should reflect time-averaging because of the slow syenite cooling, the data does not necessarily exclude the possibility of large variations of the field during the late Ediacaran-early Cambrian. This possibility is raised by an interpretation of recent paleomagnetic data from a mafic dike, thought to be part of the Grenville dike swarm emplaced at ca. 590 Ma (Kamo et al., 1995) that is cut by the Chatham-Grenville syenite (Lloyd et al., 2022), \sim 1 km from our sampling sites (Fig. 1, Supplementary Information, Supplementary Figures 5-6). Lloyd et al. (2022) interpret the

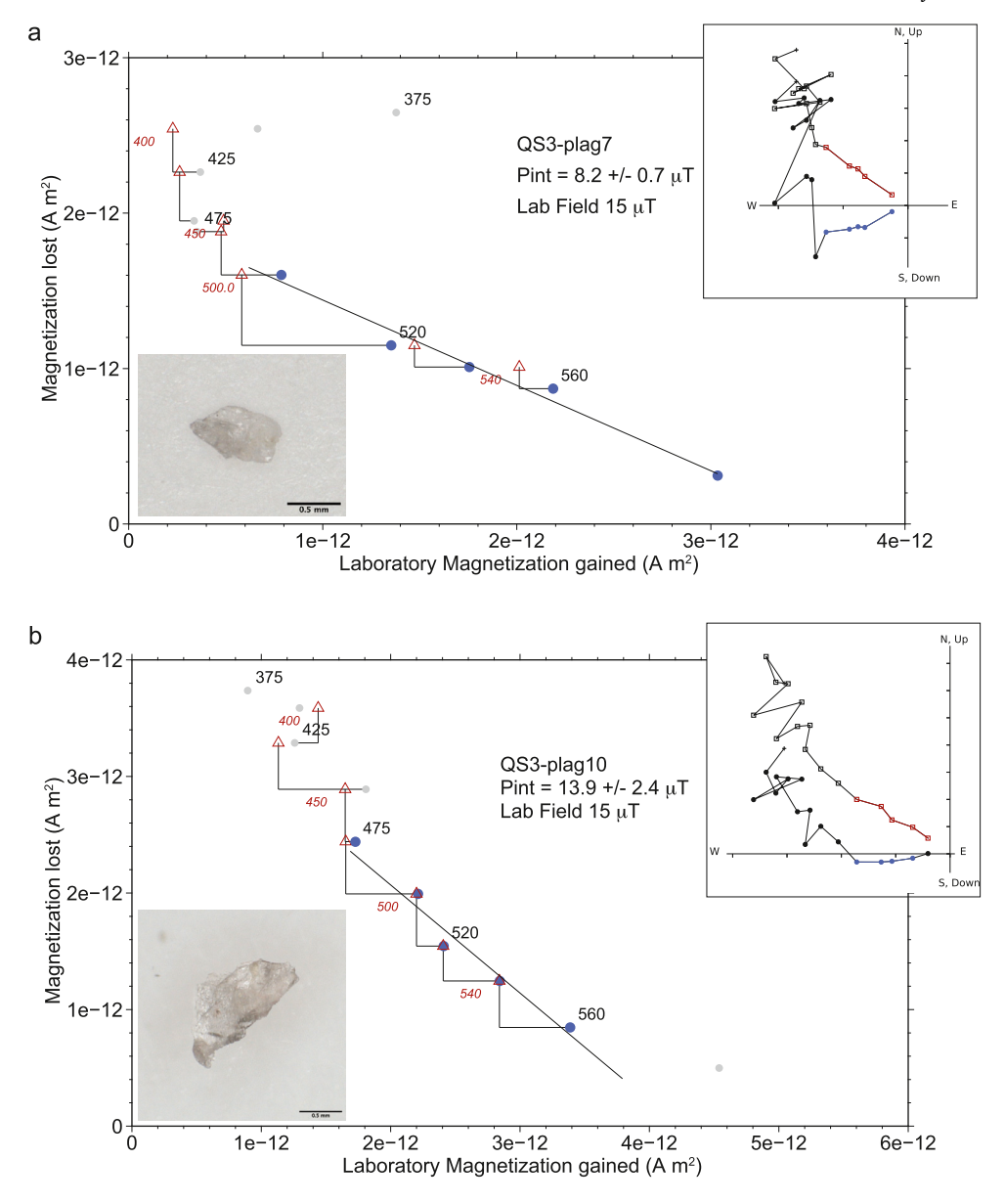


Fig. 5. Single crystal paleointensity data from Chatham-Grenville stock: Thellier-Coe data. (a) Magnetization loss (NRM) versus Laboratory Magnetization gained (TRM) (solid circles) for crystal QS3-plag7. Crystal measured shown as inset (lower left). Solid blue circles are data used in paleointensity fit. Temperatures shown are in °C. Triangles are partial thermoremanent magnetization checks. Orthogonal vector plot of field off steps also shown as inset (upper right). Solid symbols, horizontal projection of the magnetization, open squares, vertical projection of the magnetization. (b) Paleointensity data for crystal QS3-plag10, with convections as in (a).

magnetization of this dike as being thermally reset by intrusion of the syenite, and that it was slowly cooled, yielding a time-averaged field value. Three Thellier analyses reported in Lloyd et al. (2022) yield a relatively low virtual dipole moment of $0.94\pm0.16\times10^2$ A m^2 . However, the authors interpret the strong bulk magnetization as recording a lightning strike. Rocks hit by lightning are typically excluded from paleomagnetic studies because the high magnetizations imparted represent fields that can exceed the coercivities of all magnetic grains in a sample. Using careful demagnetization data, Lloyd et al. (2022) argue that an ancient magnetization direction can be isolated at high demagnetization levels.

The rock record does not appear to support the interpretation that the dike was baked and remained at temperatures of at least 590 $^{\rm o}{\rm C}$ long enough to provide a time average of the magnetic field. These temperatures are of lower amphibolite facies grade. With highly reactive mineral assemblages in a mafic dike, and excluding the absence of water in this upper crustal setting, formation of amphibolite is expected

(e.g., Passarella et al., 2017), but not reported by Lloyd et al. (2022). In our field work, we observed a covered interval between the dike and poorly exposed syenite making the exact nature of the contact uncertain. These observations, together with the lack of a formal contact test (Supplementary Information), lead us to conclude that if the dike was reheated, the peak temperature at the site of paleomagnetic sampling might have been much lower than 590 °C and/or heating might have had a shorter duration than postulated by Lloyd et al. (2022). This opens the possibility that the dike paleointensity records a higher frequency variation not seen in the syenite data because of temporal averaging. But the unblocking temperatures reported in Lloyd et al. (2022) suggest the presence of hematite which could hold a chemical remanence or thermochemical remanence (Dunlop and Özdemir, 1997), which would in general result in an underestimate of any ambient field strength (Smirnov and Tarduno, 2005). Moreover, because of the dike's multidomain magnetic carriers and the likelihood of a lower temperature thermal resetting, the paleointensity data probably reflect

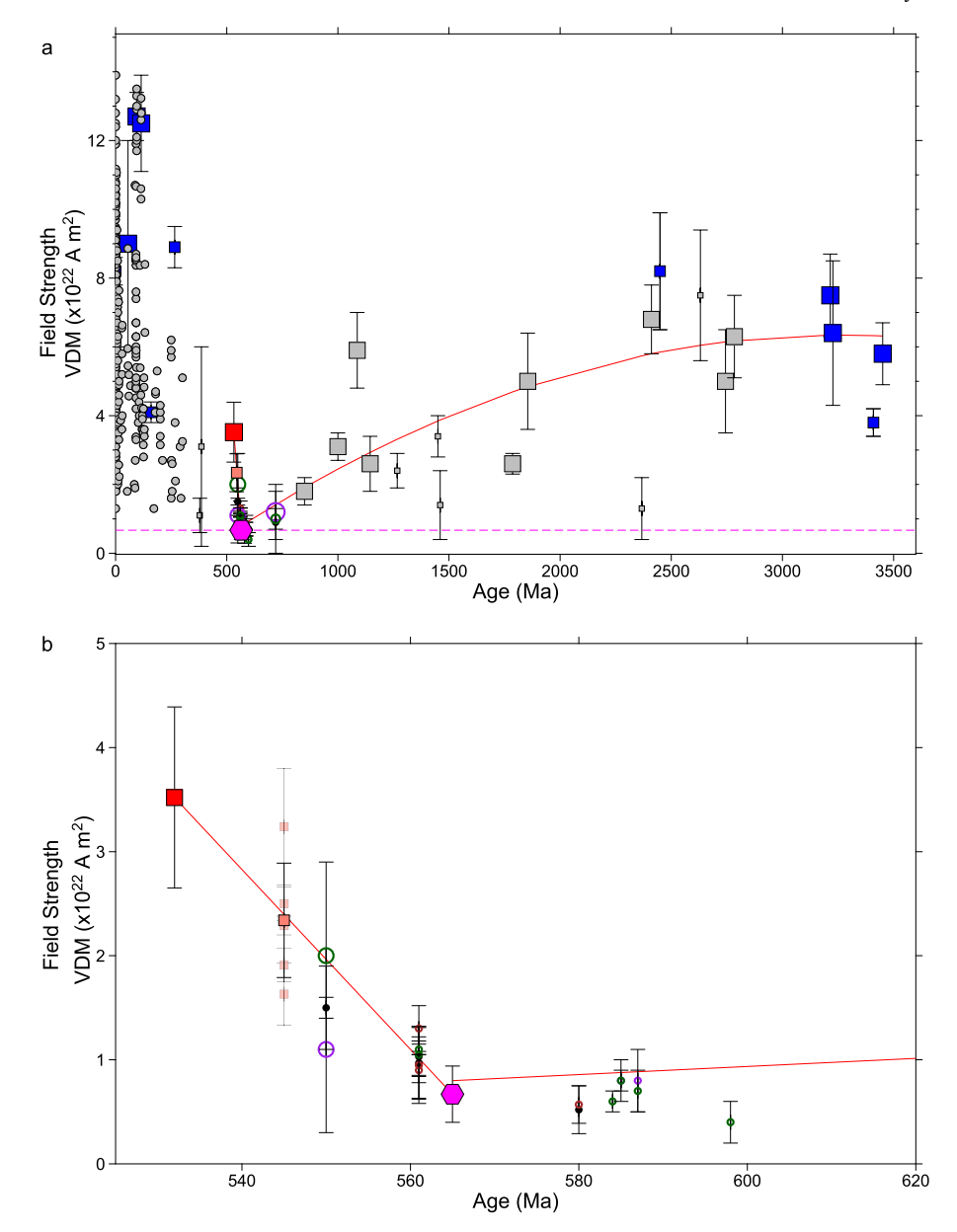


Fig. 6. Paleointensity history. (a) Paleointensity evolution with time constrained by select Thellier (thermal) single-crystal paleointensity (SCP) studies (blue squares) and bulk rock studies (gray squares) updated from Bono et al. (2019) and Zhou et al. (2022). Large squares: time-averaged paleomagnetic dipole moments (PDMs). Small squares: virtual dipole moments (VDMs). Gray circles: select Phanerozoic VDMs from Bono et al. (2019). Salmon square: average paleointensity from Chatham-Grenville syenite SCP data reported here. Smaller size of the symbol reflects the smaller number of determinations relative to Bono et al. (2019) and Zhou et al. (2022). Purple hexagon: Ediacaran ultra-low PDM from Bono et al. (2019). Red square: Early Cambrian PDM from Zhou et al. (2022). Non-Thellier method results (non-thermal and thermal) shown by open circles and their sizes are weighted by the number of cooling units as follows: green, microwave method; purple, Shaw method; brown, Wilson method; Thellier thermal results shown by black filled symbol (see Thallner et al., 2021a,b, 2022 for these results). The purple dashed line is the ultra-low Ediacaran PDM defined by Sept Îles intrusive rocks (Bono et al., 2019). Precambrian field evolution model (red line, 3450 Ma to 565 Ma) is a weighted second-order polynomial regression of field strengths from Bono et al. (2019); the 565 to 532 Ma trend (red line) is from Zhou et al. (2022). Uncertainties shown are 1σ. (b) Expansion of (a) highlighting 530 to 620 Ma interval. Solid salmon square: averaged syenite SCP data; whereas light salmon squares are the individual syenite SCP data. Uncertainties are 1σ.

a multidomain pTRM tail effect (Xu and Dunlop, 1994; Shcherbakova et al., 2000) and not a true paleofield strength (Supplementary Figure 7). The lightning strike magnetization appears to have obscured these effects (Supplementary Information).

Ultimately we exclude the dike data because of the likelihood of a pTRM tail (Supplementary Information). However, we note that paleomagnetic data from the Cambrian (Li et al., 2023) suggest high frequency geomagnetic fluctuations on a time scale of tens-of-thousands of years occurred while the inner core was small. These Cambrian variations are to date defined only in directions (i.e., reversal frequency and

dipolarity) rather than field strength. Overall, more data are needed from the Cambrian to further explore potential field variations.

4.4. Implications for paleointensity and core history

As noted above, the SCP values from the syenite further support the conclusion of Zhou et al. (2022) that by the latest Ediacaran to early Cambrian the field was renewed, consistent with inner core growth. Moreover, the paleointensity history interpretation of Zhou et al. (2022) supplemented with the new syenite values has implications for core

processes. Specifically, Christensen and Aubert (2006) suggested that magnetic field inside the core B could be represented by the scaling as follows:

$$B \approx 0.9 \mu^{1/2} \rho^{1/6} \left(\frac{g_o Q_B D}{4\pi r_0 r_i} \right)^{1/3} \tag{1}$$

where μ is magnetic permeability, ρ is density, Q_B is buoyancy flux (Methods), D is the shell thickness, and r_o and r_i are the outer and inner core radii, respectively. This scaling suggests the magnetic field strength mainly depends on buoyancy flux and size of the dynamo region, given that thresholds of rotation rate and Coriolis force are met.

The available paleointensity history to date suggests the field increased by a factor of ~5 between 565 and 532 Ma, and if the convective region was approximately constant (i.e., for small inner core sizes) this implies a factor of 125 increase in buoyancy flux according to the scaling relationship above (eqn. (1)), other things being equal. However, this increase in field strength might still fall short of levels that characterize the Phanerozoic geodynamo and a larger inner core. The long-term average field strength of the geodynamo is itself contentious. Some prefer a value of 4-5 x 10 ²² A m² (e.g., Tauxe and Staudigel, 2004). Others note the potential for rock magnetic bias toward low values (Smirnov and Tarduno, 2003, 2005; Ferk et al., 2012; Smirnov et al., 2017), and/or phenomenological arguments that a low field value would be associated with higher than observed secular variation and excursional behavior (Guyodo and Valet, 1999) seemingly inconsistent with the history of the geodynamo inferred from directional data (Tarduno and Smirnov, 2004). These arguments would favor a long-term average value closer to the present day field strength near 8 x $10^{22}\ A$ m². Subsequent considerations of Mesozoic to Recent data appear to favor a value between 5 and 6 x 10²² A m² (Kulakov et al., 2019; Bono et al., 2022), although this depends critically on the balance of time intervals represented by superchrons during which the field strength is relatively high (Tarduno et al., 2001, 2002) and time intervals of higher reversal frequency when the field is weaker (Tarduno and Cottrell, 2005; Tauxe et al., 2013). In any case, the Cambrian field intensity from Zhou et al. (2022) of $3.5 \times 10^{22} \text{ A m}^2$ is still slightly below even the lower bounds on Mesozoic-Recent longterm mean field strength, which hints that the inner core had not yet grown large enough to have buoyancy effects comparable to today. This is consistent with the interpretation of recently reported paleomagnetic data from southern China which show intervals of field instability in the late Cambrian (Li et al., 2023).

We also note that the new syenite-plagioclase data support a relatively rapid increase in field strength in the earliest Cambrian (Zhou et al., 2022) which could signal an episode of more rapid initial growth of the inner core (Labrosse, 2003), possibly also bearing on questions of inner core nucleation processes (Huguet et al., 2018; Sun et al., 2022; Wilson et al., 2023). More studies are needed, and our new results suggest that plagioclase from syenites should be considered as a future target for new SCP investigations. Overall, the available time-averaged data provides a foundation and motivation for further studies to refine paleointensity history during the critical Ediacaran to Cambrian time transition to gain insight into potential onset of inner core growth and changing buoyancy flux.

5. Methods

5.1. Field sampling

Fresh syenite samples measured here were collected in 2014 at the following locations: QS-2, N 45 o 40.142 $^\circ$, W 74 o 34.753 $^\circ$; QS-3 and QS-4: separated by approximately 1 m at N 45 o 40.147 $^\circ$, W 74 o 34.755 $^\circ$.

5.2. Geochronology

Zircon crystals were concentrated using traditional magnetic and density separation techniques. Individual grains were hand-picked under a binocular microscope, mounted in epoxy resin, and polished to expose the interior of the grains prior to cathodoluminescence (CL) imaging using a Hitachi S-3400N secondary electron microscope (SEM) equipped with a Gatan Chroma CL2 system at the Arizona Laserchron Center (ALC). U-Pb geochronologic analyses were conducted by laser ablation-inductively coupled plasma mass spectrometry (LA-ICPMS) at the ALC, using a Teledyne Iridia laser ablation system coupled to a Thermo Element2 ICP-MS. Instrumental bias, drift, and inter-element fractionation corrections were performed by the standard-sample bracketing (SSB) method, using zircon crystals from the FC-1 locality of the Duluth Gabbro with a well-established $^{206}\text{Pb}/^{238}\text{U}$ age of 1095.97 \pm 0.22 Ma and $^{207}\text{Pb}/^{206}\text{Pb}$ of 1099.96 \pm 0.58 Ma obtained using CA-ID-TIMS (Ibañez-Mejia and Tissot, 2019) as primary reference material. U-Pb analyses were conducted using a laser-beam diameter of 30 μm and by hopping between the ²³⁸U, ²³²Th, ^{208,207,206}Pb, ²⁰⁴(Pb+Hg) and ²⁰²Hg peaks using a discrete-dynode secondary electron multiplier. Data collection, processing, and uncertainty calculations follow the approach of Pullen et al. (2018). To assess the accuracy of our dates, fragments from an in-house Sri Lankan zircon megacryst with a well-established ID-TIMS age of 555.86 \pm 0.68 Ma (Wang et al., 2022) were analyzed repeatedly throughout the duration of our analytical session. The calculated mean age for this secondary reference zircon material was 558.9 \pm 4.3/6.8 Ma (2 σ , n=13, MSWD=0.6), supporting the accuracy of our U-Pb data within reported uncertainties (see Supplementary Figure 4). Mean dates discussed throughout the text are weighted mean 206 Pb/ 238 U values, and uncertainties are presented in the form \pm X/Y, where X and Y stand for different levels of uncertainty propagation as follows: X is internal analytical (random) uncertainty only, whereas Y is the total uncertainty that combines the analytical uncertainty and external (systematic) uncertainties. The internal uncertainty is appropriate when comparing data obtained using the same methods and the same primary reference material, while the propagated (internal + external) uncertainty should be used when comparing our data with U-Pb results obtained using other method and/or different isotopic decay systems (e.g., K-Ar). The external (systematic) uncertainty during our session was 0.94% for the ²⁰⁶Pb/²³⁸U values, which includes uncertainty of the ID-TIMS date for the primary reference material, SSB normalization uncertainty, and ²³⁸U decay constant uncertainty (see Pullen et al. (2018) for further details).

5.3. Rock magnetism and scanning electron microscopy

Magnetic hysteresis curves and first order reversal curve (FORC) diagrams were measured using the Princeton Measurements Alternating Gradient Force Magnetometer in the Paleomagnetic Laboratories of the University of Rochester. Averaging times of 1 second were used to measure hysteresis curves. Remanence was measured a minimum of 3 times for each sample and signals were stacked and smoothed utilizing a Savitsky-Golay filter with a window of 50 points and 3rd order polynomial. First order reversal curves were processed with ForcSensei (Heslop et al., 2020) using the following VARIFORC smoothing factors: Sc0 = Sc1 = Su0 = Su1 = 2, λ =0.1. We investigated magnetic mineralogy and domain states using a Zeiss Auriga scanning electron microscope with energy dispersive X-ray analysis (EDS) at the University of Rochester Integrated Nanosystems Center. EDS data were used to identify titanomagnetite/magnetite grains with different Ti and Fe concentrations.

5.4. Paleointensity

Analyses follow single crystal paleointensity methods (Tarduno et al., 2006). Plagioclase crystals are rare in the syenite samples and

best represented in OS3, which became the focus of our investigation. Crystals were separated from the QS3 sample and mounted using nonmagnetic adhesives in 2 mm fused quartz boxes for measurement using the ultrasensitive William S. Goree Inc. (WSGI) 3 component DC SQUID magnetometer in the magnetically shielded room at the University of Rochester (ambient field <200 nT). The nonmagnetic nature of the mounting materials was confirmed in interlaboratory tests using the scanning SQUID microscope of AIST, Japan (Tarduno et al., 2020). Samples were heated using a Synrad v20 CO₂ laser (Tarduno et al., 2007), with calibrations using IR pyrometers (e.g., O'Brien et al., 2020). For initial TTRM experiments (Tarduno et al., 2012), an arbitrary applied field is chosen (60 μ T in this case). For subsequent full Thellier analyses, the applied field is adjusted to be closer to the paleointensity value predicted by the TTRM results. Paleointensity selection criteria follow those of Cottrell and Tarduno (2000); Bono et al. (2019) and Zhou et al. (2022).

5.5. Geodynamo

We note that Q_B defined by Christensen and Aubert (2006) is in units of mass/time or kg/s.

CRediT authorship contribution statement

Tinghong Zhou: Writing – review & editing, Writing – original draft, Investigation, Formal analysis. Mauricio Ibañez-Mejia: Writing – review & editing, Writing – original draft, Investigation, Formal analysis, Conceptualization. Richard K. Bono: Writing – review & editing, Investigation. Rory D. Cottrell: Writing – review & editing, Visualization, Investigation, Formal analysis, Data curation. Wouter Bleeker: Writing – review & editing, Investigation. Kenneth P. Kodama: Writing – review & editing, Conceptualization. Wentao Huang: Writing – review & editing, Investigation. Eric G. Blackman: Writing – review & editing, Investigation. Francis Nimmo: Writing – review & editing, Investigation. Aleksey V. Smirnov: Writing – review & editing, Formal analysis, Conceptualization. John A. Tarduno: Writing – review & editing, Writing – original draft, Validation, Supervision, Funding acquisition, Formal analysis, Conceptualization.

Declaration of competing interest

The authors declare that they have no known competing financial interests or personal relationships that could have appeared to influence the work reported in this paper.

Data availability

Data presented in this manuscript is available via FigShare: https://doi.org/10.6084/m9.figshare.24639186.

Acknowledgements

This work was supported by NSF grant 1828817 to J.A.T. We thank Sandra Kamo for discussions about the ages of the Ottawa-Bonnechere Graben syenites. We also thank Allison Lloyd, Yoseph M. Dres and Ryan Goss for magnetic hysteresis measurements. M.I-M and the Arizona LaserChron Center acknowledge support by NSF award EAR-2050246. Wouter Bleeker's contribution supported by the GSC's Targeted Geoscience Initiative (NRCan Contribution #20230401). We thank Ken Buchan and the journal reviewers (Jerome Gattacceca and an anonymous reviewer) for their helpful comments.

Appendix A. Supplementary material

Supplementary material related to this article can be found online at $\frac{https:}{doi.org/10.1016/j.epsl.2024.118758}$.

References

- Bleeker, W., Dix, G.R., Davidson, A., LeCheminant, A., 2011. Tectonic evolution and sedimentary record of the Ottawa-Bonnechere graben: examining the Precambrian and Phanerozoic history of magmatic activity, faulting, and sedimentation. In: Geological Association of Canada Guidebook to Field Trip 1A. 98 p.
- Bono, R.K., Paterson, G.A., van der Boon, A., Engbers, Y.A., Grappone, J.M., Handford, B., Hawkins, L.M.A., Lloyd, S.J., Sprain, C.J., Thallner, D., Biggin, A.J., 2022. The PINT database: a definitive compilation of absolute palaeomagnetic intensity determinations since 4 billion years ago. Geophys. J. Int. 229, 522–545.
- Bono, R.K., Tarduno, J.A., 2015. A stable Ediacaran Earth recorded by single silicate crystals of the ca. 565 Ma Sept-Îles intrusion. Geology 43, 131–134.
- Bono, R.K., Tarduno, J.A., Nimmo, F., Cottrell, R.D., 2019. Young inner core inferred from Ediacaran ultra-low geomagnetic field intensity. Nat. Geosci. 12, 143–147.
- Christensen, U.R., Aubert, J., 2006. Scaling properties of convection-driven dynamos in rotating spherical shells and application to planetary magnetic fields. Geophys. J. Int. 166. 97–114.
- Cottrell, R.D., Tarduno, J.A., 1999. Geomagnetic paleointensity derived from single plagioclase crystals. Earth Planet. Sci. Lett. 169. 1–5.
- Cottrell, R.D., Tarduno, J.A., 2000. In search of high-fidelity geomagnetic paleointensities: a comparison of single plagioclase crystal and whole rock Thellier-Thellier analyses. J. Geophys. Res. 105, 23,579–23,594.
- Davies, C.J., et al., 2022. Dynamo constraints on the long-term evolution of Earth's magnetic field strength. Geophys. J. Int. 228, 316.
- Driscoll, P., 2016. Simulating 2 Ga of geodynamo history. Geophys. Res. Lett. 43, 5680-5687.
- Dunlop, D.J., 2002. Theory and application of the Day plot (Mrs/Ms versus Hcr/Hc) 1. Theoretical curves and tests using titanomagnetite data. J. Geophys. Res. 107. EPM 4-1–EPM 4-22.
- Dunlop, D.J., Özdemir, Ö., 1997. Rock Magnetism, Fundamentals and Frontiers. Cambridge University Press, New York, NY.
- Dunlop, D.J., Zhang, B.X., Özdemir, Ö., 2005. Linear and nonlinear Thellier paleointensity behavior of natural minerals. J. Geophys. Res. 110, B01103.
- Ferk, A., Denton, J.S., Leonhardt, R., Tuffen, H., Koch, S., Hess, K.U., Dingwell, D.B., 2012. Paleointensity on volcanic glass of varying hydration states. Phys. Earth Planet. Inter. 208, 25–37.
- Guyodo, Y., Valet, J.-P., 1999. Global changes in intensity of the Earth's magnetic field during the past 800 kyr. Nature 399, 249–252.
- Halgedahl, S.L., Day, D., Fuller, M., 1980. The effect of cooling rate on the intensity of weak-field TRM in single-domain magnetite. J. Geophys. Res. 85, 3690–3698.
- Hanson, R.E., Puckett Jr., R.E., Keller, G.R., Brueseke, M.E., Bulen, C.L., Mertzman, S.A., McCleery, D.A., 2013. Intraplate magmatism related to opening of the southern Iapetus Ocean: Cambrian Wichita Igneous Province in the southern Oklahoma Rift Zone. Lithos 174, 57–70.
- Heslop, D., Roberts, A.P., Oda, H., Zhao, X., Harrison, R.J., Muxworthy, A.R., Hu, P.-X., Sato, T., 2020. An automatic model selection-based machine learning framework to estimate FORC distributions. J. Geophys. Res. 125, e2020JB020418.
- Higgins, M.D., 1985. Geochemical evolution of the Chatham-Grenville stock. Can. J. Earth Sci. 22, 872–880.
- Higgins, M.D., 2005. A new interpretation of the structure of the Sept Iles Intrusive suite, Canada. Lithos 83, 199–213.
- Huguet, L., Van Orman, J.A., Hauck, S.A., Willard, M.A., 2018. Earth's inner core nucleation paradox. Earth Planet. Sci. Lett. 487, 9–20.
- Ibañez-Mejia, M., Tissot, F.L.H., 2019. Extreme Zr stable isotope fractionation during magmatic fractional crystallization. Sci. Adv. 5, eaax8648.
- Kamo, S.L., Krogh, T.E., Kumarapeli, P.S., 1995. Age of the Grenville dyke swarm, Ontario-Quebec: implications for the timing of Iapetus rifting. Can. J. Earth Sci. 32, 272, 280
- Kulakov, E.V., Sprain, C.J., Doubrovine, P.V., Smirnov, A.V., Paterson, G.A., Hawkins, L., Fairchild, L., Piispa, E.J., Biggin, A.J., 2019. Analysis of an updated paleointensity database (QPI-PINT) for 65–200 Ma: implications for the long-term history of dipole moment through the Mesozoic. J. Geophys. Res. 124, 9999–10022.
- Labrosse, S., 2003. Thermal and magnetic evolution of the Earth's core. Phys. Earth Planet. Inter. 140, 127–143.
- Li, Y.-X., Tarduno, J., Jiao, W., Liu, X., Peng, S., Xu, S., Yang, A., Yang, Z., 2023. Late Cambrian geomagnetic instability after the onset of inner core nucleation. Nat. Commun. 14, 4596.
- Lloyd, S.J., Biggin, A.J., Paterson, G.A., McCausland, P.J.A., 2022. Extremely weak early Cambrian dipole moment similar to Ediacaran: evidence for long-term trends in geomagnetic field behaviour? Earth Planet. Sci. Lett. 595, 117757.
- Malka, E., Stevenson, R.K., David, J., 2000. Sm-Nd geochemistry and U-Pb geochronology of the Mont Rigaud stock, Quebec, Canada: a late magmatic event associated with the formation of the Iapetus rift. J. Geol. 108, 569–583.
- McCausland, P.J.A., Van der Voo, R., Hall, C.M., 2007. Circum-Iapetus paleogeography of the Precambrian-Cambrian transition with a new paleomagnetic constraint from Laurentia. Precambrian Res. 156. 125–152.
- Nimmo, F., 2015. In: Schubert, G. (Ed.), Treatise on Geophysics, 2nd edition. Elsevier.
- O'Brien, T., Tarduno, J.A., Anand, A., Smirnov, A.V., Blackman, E.G., Carroll-Nellenback, J., Krot, A.N., 2020. Arrival and magnetization of carbonaceous chondrites in the asteroid belt before 4562 million years ago. Commun. Earth Environ. 1, 54.

- Passarella, M., Mountain, B.W., Seward, T.M., 2017. Experimental simulations of basalt-fluid interaction at supercritical hydrothermal condition (400 °C 500 bar). Proc. Earth Planet. Sci. 17, 770–773.
- Prevot, M., Mattern, E., Camps, P., Daignieres, M., 2000. Evidence for a 20^o tilting of the Earth's rotation axis 110 million years ago. Earth Planet. Sci. Lett. 179, 517–528.
- Pullen, A., Ibañez-Mejia, M., Gehrels, G.E., Giesler, D., Pecha, M., 2018. Optimization of a laser ablation-single collector-inductively coupled plasma-mass spectrometer (Thermo Element 2) for accurate, precise, and efficient zircon U-Th-Pb geochronology. Geochem. Geophys. Geosyst. 19, 3689–3705.
- Shcherbakova, V., Bakhmutov, V.G., Thallner, D., Shcherbakov, V.P., Zhidkov, G.V., Biggin, A.J., 2020. Ultra-low palaeointensities from East European Craton, Ukraine support a globally anomalous palaeomagnetic field in the Ediacaran. Geophys. J. Int. 220, 1928–1946.
- Shcherbakova, V.V., Shcherbakov, V.P., Heider, F., 2000. Properties of partial thermoremanent magnetization in pseudosingle domain and multidomain magnetite grains. J. Geophys. Res. 105, 767–781.
- Smirnov, A.V., Kulakov, E.V., Foucher, M.S., Bristol, K.E., 2017. Intrinsic paleointensity bias and the long-term history of the geodynamo. Sci. Adv. 3, e1602306.
- Smirnov, A.V., Tarduno, J.A., 2003. Magnetic hysteresis monitoring of Cretaceous submarine basaltic glass during Thellier paleointensity experiments: evidence for alteration and attendant low field bias. Earth Planet. Sci. Lett. 206, 571–585.
- Smirnov, A.V., Tarduno, J.A., 2005. Thermochemical remanent magnetization in Precambrian rocks: are we sure the geomagnetic field was weak? J. Geophys. Res. 110, B06103.
- Stephenson, J., Tkalčić, H., Sambridge, M., 2021. Evidence for the innermost inner core: robust parameter search for radially varying anisotropy using the neighborhood algorithm. J. Geophys. Res. 126, e2020JB020545.
- Sun, Y., Zhang, F., Mendelev, M.I., Wentzcovitch, R.M., Hoe, K.-M., 2022. Two-step nucleation of the Earth's inner core. Proc. Natl. Acad. Sci. USA 119, e2113059119.
- Tarduno, J.A., 2009. Geodynamo history preserved in single silicate crystals: origins and long-term mantle control. Elements 5, 217–222.
- Tarduno, J.A., Cottrell, R.D., 2005. Dipole strength and variation of the time-averaged reversing and nonreversing geodynamo based on Thellier analyses of single plagioclase crystals. J. Geophys. Res. 110, B11101.
- Tarduno, J.A., Cottrell, R.D., Smirnov, A.V., 2001. High geomagnetic field intensity during the mid-Cretaceous from Thellier analyses of single plagioclase crystals. Science 291, 1779–1783.
- Tarduno, J.A., Cottrell, R.D., Smirnov, A.V., 2002. The Cretaceous superchron geodynamo: observations near the tangent cylinder. Proc. Natl. Acad. Sci. 99, 14,020–14,025.
- Tarduno, J.A., Cottrell, R.D., Smirnov, A.V., 2006. The paleomagnetism of single silicate crystals: recording the geomagnetic field during mixed polarity intervals. Rev. Geophys. 44, RG1002.
- Tarduno, J.A., Cottrell, R.D., Watkeys, M.K., Bauch, D., 2007. Geomagnetic field strength 3.2 billion years ago recorded by single silicate crystals. Nature 446, 657–660.
- Tarduno, J.A., Cottrell, R.D., Nimmo, F., Hopkins, J., Voronov, J., Erickson, A., Blackman, E., Scott, E.R.D., McKinley, R., 2012. Evidence for a dynamo in the main group pallasite parent body. Science 338, 939–942.
- Tarduno, J.A., Cottrell, R.D., Bono, R.K., Oda, H., Davis, W.J., Fayek, M., Erve, O.v.'t., Francis, N., Huang, W., Thern, E.R., Fearn, S., Mitra, G., Smirnov, A.V., Blackman,

- E.G., 2020. Paleomagnetism indicates that primary magnetite in zircon records a strong Hadean geodynamo. Proc. Natl. Acad. Sci. USA 117, 2309–2318.
- Tarduno, J.A., Smirnov, A.V., 2001. Stability of the Earth with respect to the spin axis for the last 130 million years. Earth Planet. Sci. Lett. 184, 549–553.
- Tarduno, J.A., Smirnov, A.V., 2004. The paradox of low field values and the long-term history of the geodynamo. In: Channell, J.E.T., Kent, D.V., Lowrie, W., Meert, J.G. (Eds.), Timescale of the Paleomagnetic Field (Dedicated to N.D. Opdyke). In: AGU Geophysical Monograph, vol. 145, pp. 75–84.
- Tauxe, L., Gee, J.S., Steiner, M.B., Staudigel, H., 2013. Paleointensity results from the Jurassic: new constraints from submarine basaltic glasses of ODP Site 801C. Geochem. Geophys. Geosyst. 14, 4718–4733.
- Tauxe, L., Staudigel, H., 2004. Strength of the geomagnetic field in the Cretaceous Normal Superchron: new data from submarine basaltic glass of the Troodos Ophiolite. Geochem. Geophys. Geosyst. 5, Q02H06.
- Thallner, D., Biggin, A.J., Halls, H.C., 2021a. An extended period of extremely weak geomagnetic field suggested by palaeointensities from the Ediacaran Grenville Dykes (SE Canada). Earth Planet. Sci. Lett. 568, 117025.
- Thallner, D., Biggin, A.J., McCausland, P.J., Fu, R.R., 2021b. New paleointensities from the Skinner Cove Formation, Newfoundland, suggest a changing state of the geomagnetic field at the Ediacaran-Cambrian transition. J. Geophys. Res. 126, e2021.JB022292.
- Thallner, D., Shcherbakova, V.V., Bakhmutov, V.G., Shcherbakov, V.P., Zhidkov, G.V., Poliachenko, I.B., Biggin, A.J., 2022. New palaeodirections and palaeointensity data from extensive profiles through the Ediacaran section of the Volyn Basalt Province (NW Ukraine). Geophys. J. Int. 231, 474–492.
- Wall, C.J., Hanson, R.E., Mark Schmitz, M., Price, J.D., Donovan, R.N., Boro, J.R., Eschberger, A.M., Toews, C.E., 2021. Integrating zircon trace-element geochemistry and high- precision U-Pb zircon geochronology to resolve the timing and petrogenesis of the Late Ediacaran-Cambrian Wichita igneous province, Southern Oklahoma Aulacogen, USA. Geology 49, 268–272.
- Wang, J.W., Gehrels, G., Kapp, P., Sundell, K., 2022. Evidence for regionally continuous Early Cretaceous sinistral shear zones along the western flank of the Coast Mountains, coastal British Columbia, Canada. Geosphere 19, 139–162.
- Wilson, A.J., Alfé, D., Walker, A.M., Davies, C.J., 2023. Can homogeneous nucleation resolve the inner core nucleation paradox? Earth Planet. Sci. Lett. 614, 118176.
- Xu, S., Dunlop, D.J., 1994. Theory of partial thermoremanent magnetization in multidomain grains: 2. Effect of microcoercivity distribution and comparison with experiment. J. Geophys. Res. 99, 9025–9033.
- Yu, Y., 2011. Importance of cooling rate dependence of thermoremanence in paleointensity determination. J. Geophys. Res. 116, B09101.
- Zhang, Y., Swanson-Hysell, N.L., Avery, M.S., Fu, R.R., 2022. High geomagnetic field intensity recorded by anorthosite xenoliths requires a strongly powered late Mesoproterozoic geodynamo. Proc. Natl. Acad. Sci. USA 119, e2202875119.
- Zhou, T., Tarduno, J.A., Nimmo, F., Cottrell, R.D., Bono, R.K., Ibañez-Mejia, M., Huang, W., Hamilton, M., Kodama, K.P., Smirnov, A.V., Crummins, B., Padgett, F., 2022.
 Early Cambrian renewal of the geodynamo and the origin of inner core structure.
 Nat. Commun. 13, 4161.